Contents lists available at ScienceDirect

Digital Chinese Medicine

journal homepage: http://www.keaipublishing.com/dcmed

Exploring the mechanism of myofascial trigger points deactivation by Tuina via the TGF-β1/Smad3 signaling pathway

Liya Tang[a], Xiaowei Liu[a], Jiadong Zang[b], Yuqiao Zhang[a], Xiang Feng[a], Wu Li[a], Jiangshan Li[a*]

a. School of Acupuncture, Tuina and Rehabilitation, Hunan University of Chinese Medicine, Changsha, Hunan 410208, China

b. Office of Science and Technology, Hunan University of Chinese Medicine, Changsha, Hunan 410208, China

ARTICLE INFO

Article history
Received 07 October 2025
Accepted 14 January 2026
Available online 25 March 2026

Keywords
Tuina
Pressing
Inflammation
Myofascial trigger points
Fibrosis
TGF-β1
p-Smad3

ABSTRACT

Objective To investigate whether Tuina alleviates fibrotic symptoms in myofascial trigger points (MTrPs) by regulating transforming growth factor (TGF)-β1/Smad3 signaling pathway, thereby deactivating these points.

Methods This study comprised two experimental phases. In phase 1, 27 specific pathogen-free (SPF) grade female Sprague-Dawley (SD) rats were randomized into three groups: control 1, model 1, and Tuina 1 groups. Model 1 and Tuina 1 groups underwent an 8-week MTrPs modeling protocol involving blunt impact and eccentric exercise. After successful modeling, rats in Tuina 1 group received manual pressing on nodules or cord-like taut bands on the medial aspect of the left hindlimb. Pain sensitivity and tissue stiffness were evaluated via pressure pain threshold (PPT) and soft tissue tension (STT). Muscle histopathology and fibrosis were observed using hematoxylin and eosin (HE) and Masson staining. Inflammatory factors in muscle were measured by enzyme-linked immunosorbent assay (ELISA), while immunofluorescence (IF) and Western blot (WB) were used to detect the expression levels of α-smooth muscle actin (α-SMA), collagen Ⅲ, and TGF-β1. In phase 2, 45 SPF female SD rats were randomized into five groups: control 2, model 2, Tuina 2, TGF-β1 inhibitor (TI), and Tuina + TGF-β1 agonist (Tuina + TA) groups. All groups except control 2 underwent standardized MTrPs modeling. Rats in Tuina 2 group received consistent pressing manipulation. TI group received intraperitoneal injections of oxymatrine, while Tuina + TA group received intraperitoneal injections of SRI-011381 hydrochloride followed by the same pressing protocol as Tuina 2 group. WB was used to detect the expression of collagen I, collagen III, TGF-β1, and phosphorylated-Smad3 (p-Smad3)/Smad3.

Results In phase 1, Tuina significantly improved PPT and STT in MTrPs of rats ($P < 0.01$), reversed pathological damages including disorganized muscle fiber arrangement, abnormal myocyte morphology, and exacerbated fibrosis. In addition, in MTrPs of rats in model 1 group, expression levels of nuclear factor kappa-light-chain-enhancer of activated B cells (NF-κB), interleukin (IL)-1β, IL-6, tumor necrosis factor (TNF)-α, and fibrosis markers (α-SMA, collagen I, and collagen III) were upregulated, and all exhibited a significant downward trend after Tuina intervention ($P < 0.05$ or $P < 0.01$). This indicates that the therapeutic effects of Tuina are directly associated with reduced local inflammation and fibrosis in MTrPs. In phase 2, compared with model 2 group, rats in TI and Tuina 2 groups had decreased

*Corresponding author: Jiangshan Li, E-mail: 001316@hnucm.edu.cn.

Peer review under the responsibility of Hunan University of Chinese Medicine.

DOI: 10.1016/j.dcmed.2026.02.009

Citation: TANG LY, LIU XW, ZANG JD, et al. Exploring the mechanism of myofascial trigger points deactivation by Tuina via the TGF-β1/Smad3 signaling pathway. Digital Chinese Medicine, 2026, 9(1): 103-113.

expression levels of TGF-β1 and p-Smad3/Smad3 in MTrPs, alongside reduced levels of inflammatory factors (IL-1β, IL-6, NF-κB, and TNF-α) and fibrosis markers (α-SMA, collagen I, and collagen III) ($P < 0.05$ or $P < 0.01$). When co-administered with TGF-β1 agonist, the therapeutic effects of Tuina were significantly attenuated, with rebounded TGF-β1 expression and p-Smad3/Smad3 in local MTrPs, and fibrosis and inflammatory responses were re-exacerbated ($P < 0.05$ or $P < 0.01$).

Conclusion Tuina can effectively reduce inflammatory responses and fibrosis in MTrPs tissue, and its mechanism is closely related to the inhibition of the TGF-β1/Smad3 signaling pathway, which plays a critical role in Tuina-mediated regulation of MTrPs fibrosis.

1 Introduction

Myofascial trigger points (MTrPs), which are irritable areas within muscle contraction bands that form due to sustained local muscle tension from acute/chronic injuries and overloading, remain a key cause of myofascial pain syndrome (MPS). Epidemiological study indicates that MTrPs were present in 93% of patients diagnosed with MPS [1]. Activated MTrPs could cause local muscle pain, referred pain, and autonomic dysfunction, severely impairing patients' quality of life and increasing socioeconomic burden [2]. The progression of MTrPs involved several processes, such as motor endplate irregularities, acetylcholine buildup, local circulation and energy metabolism issues, autonomic dysfunction, and release of vasoactive and inflammatory components [3]. Among these, persistent infiltration of inflammatory factors further stimulated the activation of myofibroblasts and promoted extracellular matrix (ECM) deposition, thereby causing local fibrosis at MTrPs [4].

Skeletal muscle fibrosis is characterized as the terminal pathological manifestation of various muscle diseases [5]. Study has found that localized fibrosis in MTrPs serves as a key factor leading to local hardening, functional loss, and exacerbated pain of MTrPs. Moreover, MTrPs fibrosis further aggravated circulatory disorders and solidified MTrPs [6], while inhibiting fibrosis could effectively improve local soft tissue tension (STT) of MTrPs and restore functional activities [7]. Transforming growth factor (TGF)-β1 was significantly upregulated in fibrotic tissues and acted as a key driver of tissue fibrosis [8]. It promoted the fibrotic process via both Smad pathway and non-Smad pathways [9]. Smad3 serves as a critical mediator of TGF-β1 signaling transduction. TGF-β1 acts on Smad3 to induce its phosphorylation (p-Smad3), thereby promoting myofibroblast activation and further aggravating the deposition of collagen fibers, including collagen I and collagen III, resulting in tissue scarring and fibrotic lesions [10]. Inhibiting TGF-β1/Smad3 signaling transduction can effectively reduce tissue fibrosis and promote functional recovery. Therefore, targeting the TGF-β1/Smad3 signaling pathway effectively inhibits tissue fibrosis [11].

Currently, the mainstay treatments for MTrPs involves oral administration or local injection of drugs. However, the associated drug resistance and infection risks from injections have persistently challenged patients [12]. Tuina, a non-toxic and environmentally friendly traditional Chinese medicine (TCM) therapy, has been extensively applied in treating MTrPs [13, 14]. According to TCM theory, myofascial pain associated with MTrPs is categorized as “meridian sinew disorders”, which is treated according to the principles of “pain indicating the point” and “pressing to disperse blood and Qi, thereby relieving pain” [15], demonstrating that pressing has the effect of relaxing tendons and relieving pain. A recent study in evidence-based medicine has verified that Tuina can effectively deactivate MTrPs [16]. Thus, studying the exact mechanism by which Tuina treats MTrPs is essential. Existing basic studies have shown that Tuina can effectively improve the pressure pain threshold (PPT) and relieve STT in MTrPs in rats by reducing inflammation, inhibiting acetylcholine neurotransmitter release, regulating local energy metabolism, and modulating the autonomic nervous system [17].

Research has shown that Tuina is effective in reducing inflammation and fibrosis in MTrPs [18]. Whether Tuina lowers MTrPs fibrosis by blocking the TGF-β1/Smad3 signaling pathway still warrants further confirmation. The core pathological features of human MTrPs contain locally hypersensitive nodules and palpable taut bands, accompanied by pain and dysfunction. Their formation is closely associated with muscle injury and fascial tension imbalance caused by high-load exercise. HUANG et al. [19] established a rat model of MTrPs using blunt percussion and eccentric exercise: blunt percussion induced muscle injury, while prolonged eccentric exercise was a key cause of fascial tension imbalance. Nodules and taut bands were also observed in the MTrPs model rats induced by this method [4]. Therefore, this study aims to utilize the MTrPs rat model and apply Tuina to elucidate its therapeutic effects in inhibiting the TGF-β1/Smad3 signaling pathway to alleviate the tissue fibrosis in MTrPs.

2 Materials and methods

2.1 Animals

A total of 72 specific pathogen-free (SPF) grade female Sprague-Dawley (SD) rats (8 weeks-old, weighing 250 – 280 g) , were purchased from Hunan Slack Jingda Experimental Animal Co., Ltd. [Animal Experiment License No. SCXK (Xiang) 2019-0009; Facility Use Compliance Certificate No. 430727231101162627]. All animals were kept in cages at the Laboratory Animal Center of Hunan University of Chinese Medicine, under conditions of 20 – 25 °C temperature and 50% – 70% relative humidity. All animal experiments were performed in compliance with China's national standards for animal welfare, and approval was obtained from the Laboratory Animal Ethics Committee at Hunan University of Chinese Medicine (Ethics No. LL2021102004).

2.2 Modeling and intervention

2.2.1 MTrPs model preparation and evaluation This study adopted the modified blunt impact combined with eccentric exercise method developed by HUANG et al. [19] for modeling. Eighteen rats were used as controls, receiving only inhalation anesthesia without impact. The remaining rats were subjected to the modeling process. First, the rats were trained on a treadmill set at a 0° incline, moving at 16 m per minute, for 15 min per session, once a day for a total of three times. An 8-week protocol combining blunt impact and eccentric exercise was carried out after the adaptive training for 3 d. Blunt impact was administered on the first day of each week. The rats were under anesthesia with 4% isoflurane inhalation and secured to the base of the impact apparatus. The medial thigh of their left hindlimb was exposed and marked. A 1 200 g blunt weight rod with kinetic energy of about 2.352 J was released from a height of 20 cm to hit the designated spot. On day 2, the rats were placed on a treadmill set to a – 16° incline and a speed of 16 m/min for 90 min of eccentric exercise, with mechanical and auditory stimuli applied to maintain continuous running. Control rats were housed under normal conditions. For the remaining 5 d of each week, all rats were housed normally without additional interventions. Finally, a 4-week recovery period was implemented, during which all rats received normal feeding and regular observation.

After the recovery period, the blunt impact site of the rats was palpated by researchers. Successful modeling was confirmed if marked nodules or cord-like taut bands appeared on the medial side of the left hindlimb, along with significantly lower PPT and STT values compared with controls ($P < 0.05$).

2.2.2 Grouping and intervention (i) Phase 1. The phase 1 of the study included control 1, model 1, and Tuina 1 groups ($n = 9$ each group). In both control 1 and model 1 groups, rats were anesthetized solely with 5% isoflurane inhalation, with no further interventions. Rats in Tuina 1 group were anesthetized with 5% isoflurane via inhalation, fixed in a supine position on a press manipulation stimulator. The left lower limb of the rats was palpated, and nodules or cord-like tight bands on the medial side of the left lower limb were marked with a marker pen. The parameters of the press manipulation stimulator were set as follows [18]: force (0.7 kg), frequency (10 times/min), and duration (7.5 min per session). The marked area was pressed vertically, with interventions administered once every other day for a total of seven sessions. The press-stimulation equipment was calibrated weekly using a precision load cell to ensure force accuracy (± 0.02 kg) and angle alignment (± 1°). All operators received theoretical instruction on the anatomical localization of rats and practical training on the operation of the press-stimulation device. Every intervention was conducted in a room where the temperature was maintained at 23 ± 1 °C and a 12 : 12 light-dark cycle was used to lower variability. Intervention times and animal movement were recorded in a log.

(ii) Phase 2. The phase 2 of the study included control 2, model 2, Tuina 2, TGF-β1 inhibitor (TI), and Tuina + TGF-β1 agonist (Tuina + TA) groups ($n = 9$ each group). Rats in control 2, model 2, and Tuina 2 groups were subjected to the identical intervention as implemented in the phase 1. After the recovery period, rats in TI group were administered oxymatrine (MedChemExpress, USA, a TGF-β1 inhibitor) intraperitoneally (i.p.) at a dose of 10 mg/kg every other day, for a total of seven times [20]. Rats in Tuina + TA group first received an injection of SRI-011381 hydrochloride (MedChemExpress, USA, a TGF-β1 agonist) at a dose of 30 mg/kg (i.p.) every other day, for a total of seven times, followed by pressing [21].

2.3 Observation and detection indicators

2.3.1 Pressure pain threshold of MTrPs The PPT was assessed by two experimenters using a mechanical pain threshold meter on the first day after the recovery period and on the first day after the last intervention. One experimenter gently restrained the rat in a supine position with its hindlimbs extended to maintain calmness. The second experimenter palpated the modeled area to locate muscle tension bands or nodules and marked the spot. The mechanical pain threshold meter was then used to slowly press the marked area; for rats in control 1 and 2 groups, the corresponding area was pressed. The value was recorded when the rat exhibited a sudden leg withdrawal or vocalization. Each rat underwent testing three times, with a 10-min break between each test, and the mean value was recorded as the PPT for that rat.

2.3.2 STT at MTrPs STT was measured by two experimenters using a soft tissue tension meter on the first day post-modeling recovery and on the first day post-intervention. One experimenter manually restrained the rat in a supine position with hindlimbs extended to maintain calmness. The other experimenter aligned the probe with the marked site, applied vertical, uniform pressure for 3 s, then released the pressure uniformly over 3 s. The observation index used was the displacement at 0.2 kg ($D_{0.2}$) on the force-displacement curve, offering a precise assessment of muscle STT in rats. A higher $D_{0.2}$ value indicates a lower STT in rats [22]. Every rat underwent testing three times, with a 10-min break between each test, and the mean value was recorded as the STT for that rat.

2.3.3 Tissue collecting After PPT and STT measurements, rats in all groups were euthanized by intraperitoneal injection of sodium pentobarbital (150 mg/kg). From each group, three rats were randomly selected for transcardial perfusion with physiological saline until clear effluent was obtained, followed by fixation with 4% paraformaldehyde. From these perfused rats, 0.5 cm × 0.5 cm samples of nodules or cord-like taut bands were harvested from the medial thigh of the left hindlimb for subsequent hematoxylin and eosin (HE) staining, Masson staining, and immunofluorescence (IF) assays. From the remaining six non-perfused rats in each group, samples of nodules or cord-like taut bands were harvested from the same site and divided into portions for different analyses: 100 mg samples for enzyme-linked immunosorbent assay (ELISA) and 150 mg samples for Western blot (WB) analyses, respectively.

2.3.4 HE staining of MTrPs Samples from the MTrPs region were fixed in 4% paraformaldehyde, embedded in paraffin, and sectioned into 5-μm-thick slices. The sections were soaked in xylene I and II for 20 min each, then in absolute ethanol I and II for 5 min each, followed by a 5-min soak in 75% ethanol, and finally rinsed under running water. The sections were immersed in hematoxylin for 5 min, washed under running water, treated with a differentiation solution, rinsed once more, turned blue with a bluing solution, and finally washed under running water. The dehydration process involved using 85% and 95% ethanol for 5 min each. The sections were stained with eosin for 5 min, then dehydrated in three stages of absolute ethanol (5 min each), and finally cleared with two stages of xylene (5 min each). Ultimately, the sections were mounted with neutral resin. Microscopic examination was performed using an upright light microscope (Nikon Eclipse E100). Image acquisition and analysis were conducted with an imaging system (Nikon, DS-U3).

2.3.5 Masson staining of MTrPs Samples from the MTrPs region were fixed in 4% paraformaldehyde, paraffin-embedded, and sectioned into 3-μm-thick slices. The paraffin sections underwent deparaffinization and rehydration. Thereafter, they were washed under running water and then with distilled water. The nuclei were stained with Regaud's hematoxylin for 10 min, followed by a thorough water wash. After rinsing with distilled water, the sections were stained with Masson's ponceau acid fuchsin solution for 10 min and then rinsed with 2% glacial acetic acid solution. The sections were treated with 1% phosphomolybdic acid solution for 10 min for differentiation, followed by staining with a light green solution for 5 min, and rinsed again with 2% glacial acetic acid solution. Finally, the sections were dehydrated through 95% ethanol, absolute ethanol, and cleared in xylene, and mounted with neutral resin. Images were obtained using a microscope, and ImageJ was used for data analysis.

2.3.6 ELISA detection of MTrPs 100 mg of tissues from the MTrPs region were weighed, minced, and mixed with 1 mL of pre-chilled radioimmunoprecipitation assay (RIPA) buffer. The mixture was thoroughly homogenized using a tissue homogenizer on ice, then centrifuged at 12 000 rpm for 15 min at 4 °C. The supernatant was cautiously aspirated and transferred to a new centrifuge tube. The levels of inflammatory indicators in MTrPs were measured using the nuclear factor kappa-light-chain-enhancer of activated B cells (NF-κB) kit, interleukin (IL)-6 kit, IL-1β kit, and tumor necrosis factor (TNF)-α kit (Shanghai Jianglai Biotechnology Co., Ltd., China). The supernatant was added to the corresponding 96-well plates and incubated at 37 °C for 60 min. The liquid was discarded, and 100 μL of antibody working solution was added, followed by incubation at 37 °C for another 60 min. The plates were washed three times with wash buffer (1 min per wash). 100 μL of enzyme conjugate working solution was added and incubated at 37 °C for 30 min. The plates were then washed five times with wash buffer (1 min per wash). 90 μL of substrate was added and incubated at 37 °C for 15 min, followed by the addition of 50 μL of stop solution. The optical density values of each well were measured at 450 nm, and the results were determined following the standard curve.

2.3.7 IF analysis of MTrPs Samples from the MTrPs region were preserved in 4% paraformaldehyde, then deparaffinized and dehydrated through several ethanol gradients. After retrieving the antigens, the sections were washed three times with phosphate-buffered saline with Tween (PBST) for 5 min each. The samples were incubated with 10% bovine serum albumin (BSA) in a humidified environment at 37 °C for 30 min. Primary antibodies, anti-α-smooth muscle actin (α-SMA, 1 : 500; AiFang Biological, China) and anti-collagen type Ⅲ (1 : 200, Proteintech, China), were applied and incubated overnight at 4 °C. Samples were washed two times with PBST for 5 min

each on the following day. Secondary antibodies, anti-mouse IgG heavy and light chains (1 : 1 000, AiFang Biological, China) and anti-rabbit IgG heavy and light chains (1 : 1 000, AiFang Biological, China), were then added and incubated for 1 h at room temperature in the dark, then rinsed three times with PBST for 5 min each. Sections were mounted using a 4',6-diamidino-2-phenylindole (DAPI)-containing medium. Microscopic images were captured for analysis via ImageJ.

2.3.8 WB analysis of MTrPs 150 mg of tissues from the MTrPs region were collected, minced, and lysed with RIPA. Following centrifugation, the supernatant was gathered, and protein levels were measured using the bicinchoninic acid (BCA) protein assay. The protein samples underwent electrophoresis, after which they were transferred to membranes and blocked. Primary antibodies: anti-TGF-β (1 : 2 000, Affinity, China), anti-collagen I (1 : 2 000, Proteintech, USA), anti-collagen III (1 : 2 000, Proteintech, USA), anti-Smad3 (1 : 2 000, Affinity, China), anti-p-Smad3 (1 : 2 000, Affinity, China), and anti-glyceraldehyde-3-phosphate dehydrogenase (GAPDH) (1 : 10 000, Zhengneng Biotechnology, China) were incubated overnight. Corresponding secondary antibodies: anti-rabbit IgG-horseradish peroxidase (HRP) (1 : 10 000, Elabscience Biotechnology, China) and anti-mouse IgG-HRP (1 : 10 000, Elabscience Biotechnology, China) were then applied and incubated for 1 h at room temperature, followed by the analysis using a detection system. Detection was carried out using an imaging system. Image-Pro Plus 6.0 software was used to analyze the grayscale intensity of protein bands, and the relative expression levels were calculated by comparing the grayscale ratio of the target protein bands to the internal reference protein GAPDH.

2.4 Statistical analysis

Data were analyzed with SPSS 26.0, and the measurement data are expressed as mean ± standard deviation (SD). For data with a normal distribution and uniform variance, paired *t* tests were applied for within-group comparisons pre- and post-treatment, while one-way analysis of variance (ANOVA) was used for between-group comparisons. The rank-sum test was used if these conditions were not met. $P < 0.05$ was considered statistically significant.

3 Results

3.1 Effects of Tuina on PPT, STT, and histopathological architecture in MTrPs

To investigate whether Tuina can inhibit MTrPs fibrosis, we established control 1, model 1, and Tuina 1 groups. Before the intervention, the evaluation of PPT and $D_{0.2}$ in each group showed a significant reduction in both values for model 1 and Tuina 1 groups compared with control 1 group ($P < 0.01$), which indicated successful establishment of the MTrPs model. After pressing intervention, Tuina 1 group exhibited significantly increased PPT and $D_{0.2}$ values compared with model 1 group ($P < 0.01$; Figure 1A and 1B). HE staining demonstrated that muscle fibers in model 1 group were disorganized, with several round, deeply stained muscle cells observed compared with control 1 group. The number of round, deeply stained muscle cells at MTrPs in rats showed a decrease after the pressing treatment compared with model 1 group (Figure 1C). Masson staining showed that rats in model 1 group exhibited a significantly larger positive area compared with control 1 group. After pressing intervention, positive area at MTrPs was reduced ($P < 0.01$; Figure 1D and 1E).

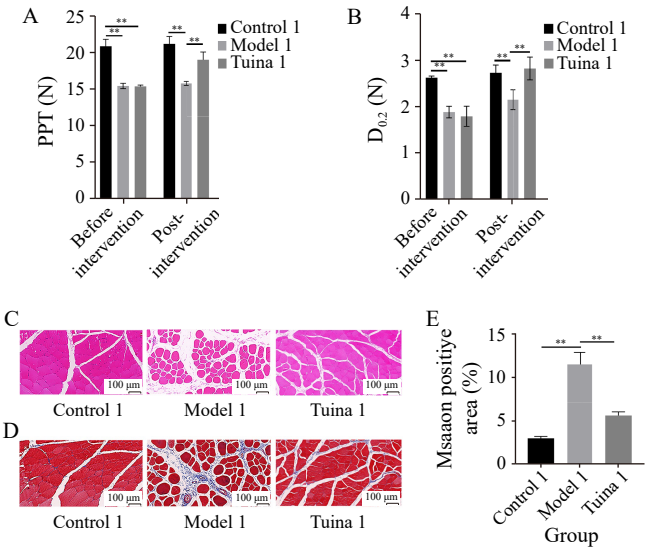

Figure 1 Comparison of PPT, STT, and histopathological changes in MTrPs of rats

A and B, evaluation of PPT and $D_{0.2}$ values of rats before and after intervention, respectively. C, HE staining images (× 200). D, Masson staining images (× 200). E, Masson positive area. $^{**}P < 0.01$.

3.2 Effects of Tuina on inflammatory cytokines and fibrotic markers expression in MTrPs

ELISA was employed to measure the inflammatory factor levels in the MTrPs of rats across different groups. Model 1 group showed a significant increase in NF-κB, IL-1β, IL-6, and TNF-α levels in the MTrPs compared with control 1 group ($P < 0.05$ or $P < 0.01$). The concentrations of NF-κB, IL-1β, IL-6, and TNF-α in MTrPs in Tuina 1 group showed a significant decrease compared with model 1 group ($P < 0.01$; Figure 2A – 2D). The expression levels of α-SMA and collagen III in MTrPs were detected using IF. In comparison with control 1 group, model 1 group showed a significant increase in expression levels of α-SMA and collagen III in MTrPs, which was decreased after Tuina

intervention ($P < 0.01$; Figure 2E – 2H). WB analysis revealed that TGF-β1 level in MTrPs was significantly higher in model 1 group compared with control 1 group ($P < 0.01$), and Tuina treatment effectively lowered it ($P < 0.01$; Figure 2I and 2J). These findings suggest that Tuina can efficiently lessen inflammation and fibrosis in MTrPs, and its anti-fibrotic effects might be linked to the modulation of TGF-β1 expression.

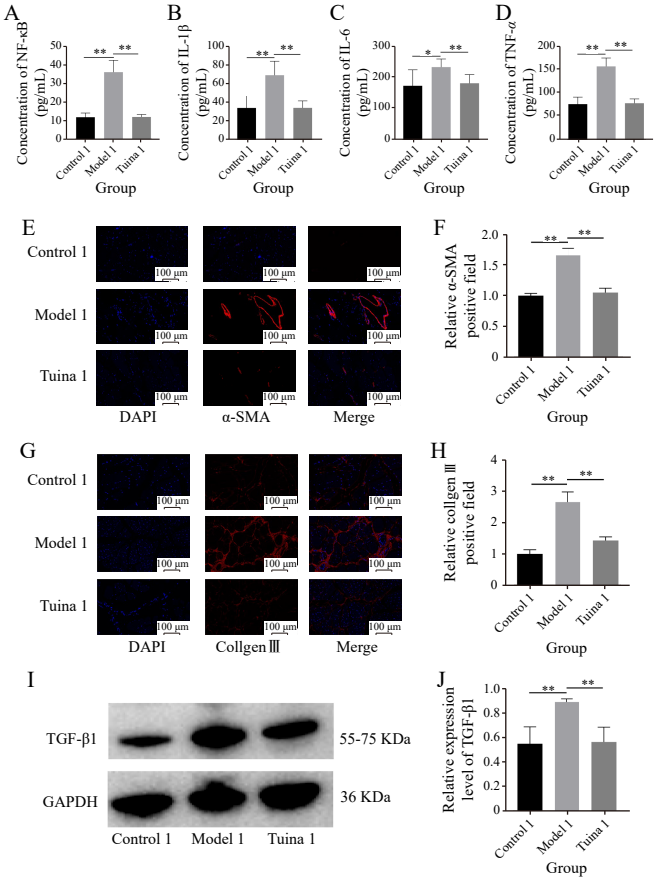

Figure 2 Comparison of inflammatory responses, fibrotic markers, and TGF-β1 expression in MTrPs of rats

A, NF-κB. B, IL-1β. C, IL-6. D, TNF-α. E, IF images of α-SMA in MTrPs (× 200). F, relative α-SMA positive field in MTrPs. G, IF images of collagen III in MTrPs (× 200). H, relative collagen III positive field in MTrPs. I, WB images of TGF-β1 in MTrPs. J, relative expression level of TGF-β1 in MTrPs. $^{*}P < 0.05$ and $^{**}P < 0.01$.

3.3 Effects of Tuina combined with TGF-β1 modulation on PPT, STT, histopathology, and inflammation in MTrPs

To further verify that Tuina alleviates MTrPs fibrosis by inhibiting TGF-β1 expression, a TGF-β1 inhibitor and a TGF-β1 agonist were added individually based on the results of the first phase of the experiment; control 2, model 2, Tuina 2, TI, and Tuina + TA groups were established. The PPT and $D_{0.2}$ values in model 2, Tuina 2, TI, and Tuina + TA groups were significantly lower than those in control 2 group ($P < 0.01$), indicating successful modeling. Following the intervention, the PPT and $D_{0.2}$ values of rats in TI and Tuina 2 groups were significantly higher than those in model 2 group ($P < 0.05$ or $P < 0.01$). Compared with Tuina 2 group, Tuina + TA group exhibited significantly lower PPT and $D_{0.2}$ values ($P < 0.05$ or $P < 0.01$; Figure 3A and 3B). HE staining results showed that rats in TI and Tuina 2 groups exhibited marked improvements in the histomorphological structure of MTrPs compared with model 2 group. In contrast, Tuina + TA group showed disorganized muscle cell arrangement with numerous round and deeply stained muscle cells in MTrPs, whose histomorphology resembled that of model 2 group (Figure 3C). ELISA demonstrated that the expression levels of NF-κB, IL-1β, IL-6, and TNF-α of rats in TI and Tuina 2 groups were decreased ($P < 0.01$). Tuina 2 group exhibited a significant decrease in NF-κB level compared with TI group ($P < 0.05$), with no significant differences in other inflammatory indicators ($P > 0.05$). In contrast, Tuina + TA group displayed increased expression levels of NF-κB, IL-1β, IL-6, and TNF-α in MTrPs compared with Tuina 2 group ($P < 0.01$ or $P < 0.05$; Figure 3D – 3G). These results indicate that Tuina alleviates pain, STT, histomorphological abnormalities, and inflammation at MTrPs by downregulating TGF-β1 expression.

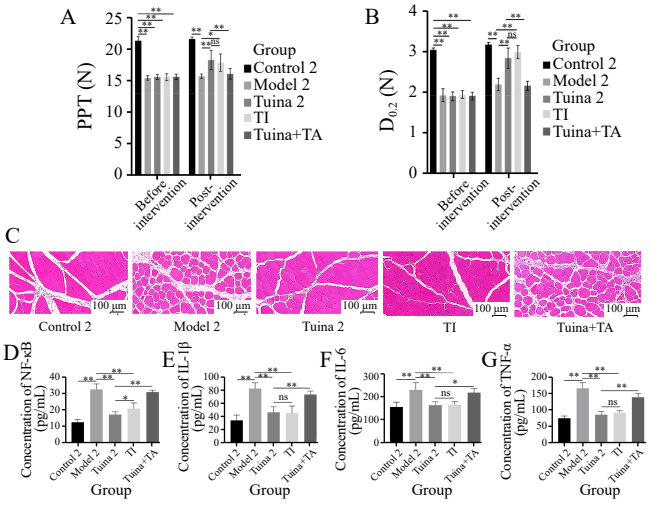

Figure 3 Comparison of PPT, STT, histomorphology, and inflammatory responses in MTrPs of rats under TGF-β1 modulation

A and B, evaluation of PPT and $D_{0.2}$ values in the five groups before and after intervention, respectively. C, HE staining of each group (× 200). D – G, concentration of NF-κB, IL-1β, IL-6, and TNF-α in MTrPs of each group, respectively. $^{ns}P > 0.05$, $^{*}P < 0.05$, and $^{**}P < 0.01$.

3.4 Effects of Tuina combined with TGF-β1 modulation on fibrotic markers and TGF-β1/Smad3 signaling in MTrPs

Masson staining showed that both Tuina 2 and TI groups exhibited a significant reduction in the positive area of

MTrPs in rats compared with model 2 group ($P < 0.01$), while no significant difference was observed between Tuina 2 and TI groups ($P > 0.05$). Compared with Tuina 2 group, Tuina + TA group showed an increased positive area in MTrPs ($P < 0.01$; Figure 4A and 4B). IF analysis revealed that α-SMA expression in MTrPs was significantly decreased in both Tuina 2 and TI groups compared with model 2 group ($P < 0.01$), with no significant differences noted between these two groups ($P > 0.05$). Moreover, α-SMA expression in MTrPs of rats was significantly increased in Tuina + TA group compared the Tuina 2 group ($P < 0.01$; Figure 4C and 4D).

WB analysis revealed that the expression levels of collagen I, collagen III, and TGF-β1 in MTrPs were significantly elevated in model 2 group compared with control 2 group ($P < 0.01$ or $P < 0.05$), and the ratio of p-Smad3/Smad3 showed a significant increase ($P < 0.01$). Following Tuina intervention or intraperitoneal injection of TI, all aforementioned parameters in MTrPs showed significant reductions ($P < 0.01$ or $P < 0.05$). However, compared with Tuina 2 group, Tuina + TA group exhibited

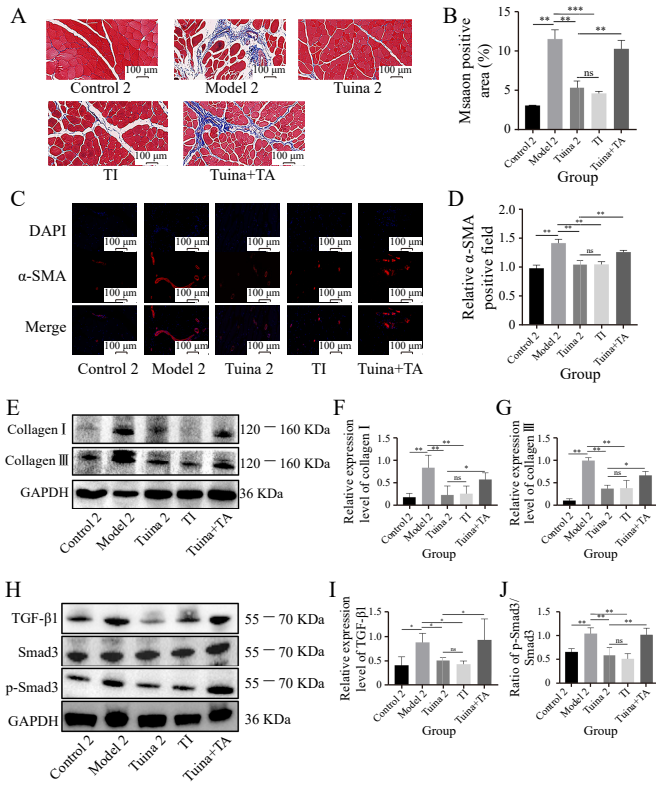

Figure 4 Comparison of fibrotic markers and TGF-β1/Smad3 signaling in MTrPs of rats under TGF-β1 modulation

A, Masson staining images of the five groups (× 200). B, Masson positive area. C, IF images of α-SMA in the MTrPs (× 200). D, relative α-SMA positive field in MTrPs. E, WB images of collagen I and collagen III in the MTrPs. F and G, relative expression levels of collagen I and collagen III in MTrPs, respectively. H, WB images of TGF-β, Smad3, and p-Smad3 in the MTrPs. I, relative expression level of TGF-β in MTrPs. J, relative ratio of p-Smad3/Smad3 in MTrPs. $^{ns}P > 0.05$, $^{*}P < 0.05$, and $^{**}P < 0.01$.

increased expression levels of collagen I, collagen III, and TGF-β1, along with a significantly elevated p-Smad3/Smad3 ratio ($P < 0.01$; Figure 4E – 4J). These findings indicate that inhibition of the TGF-β1/Smad3 pathway effectively attenuates fibrosis severity in MTrPs, with Tuina and TI injection exerting comparable therapeutic effects. Conversely, intraperitoneal administration of TGF-β1 agonist eliminates the antifibrotic effect of Tuina on MTrPs.

4 Discussion

4.1 Attenuation of inflammation and fibrosis in MTrPs rats via Tuina

Tuina has shown good efficacy in relieving adhesions and pain. As a green, drug-free TCM therapy with no toxic side effects, it exhibited excellent deactivation effects on MTrPs [23]. Muscle injury and chronic strain could lead to changes in muscle structure and function, and muscle fibrosis resulted in elevated muscle stiffness and tension, thereby causing muscle dysfunction and pain [24]. The first phase of this study found that Tuina could effectively improve the PPT and STT of MTrPs, with histopathology and reduced Masson positive area.

Study has indicated that quiescent fibroblasts in muscle tissue are transformed into myofibroblasts by sustained elevation of inflammatory cytokines at MTrPs. α-SMA, a specific marker on myofibroblast membranes, exhibited increased expression as myofibroblast abundance rose in tissue [25]. Myofibroblasts facilitated the formation of capillaries, promoting tissue repair, and regeneration that ultimately results in muscle tissue fibrosis [26]. Results from the phase 1 of this study demonstrate that Tuina significantly reduced the expression levels of inflammatory cytokines in MTrPs. Furthermore, Tuina downregulated α-SMA expression in MTrPs. In muscle, increased expression levels of collagen I and collagen III led to tissue fibrosis [27]. Previous study has demonstrated elevated levels of both collagen I and collagen III in MTrPs rats [28]. The present study found that collagen III expression in MTrPs was upregulated among rats, and Tuina effectively lowered collagen III expression at MTrPs. These findings indicate that Tuina has the potential to suppress inflammatory factor expression and reduce fibrosis.

4.2 Potential association between Tuina-mediated reduction of MTrPs fibrosis and inhibition of TGF-β1 expression

TGF-β1 exerted multiple functions in organisms and served as a key factor in activating the transformation of fibroblasts into myofibroblasts, secreting ECM, and promoting tissue fibrosis [29]. Research indicates that

specifically inhibiting TGF-β1 expression in tissues could significantly decrease tissue fibrosis [30], whereas an increase in TGF-β1 expression resulted in a notable rise in ECM [31]. Clinically, most chemical agents and natural drugs for treating fibrosis regulated TGF-β1 signal transduction and target tissue fibrosis [10]. The phase 1 of the study showed a rise in TGF-β1 expression in MTrPs, but Tuina significantly reduced TGF-β1 expression in MTrPs. These findings initially demonstrate that Tuina might decrease MTrPs fibrosis by suppressing TGF-β1 expression.

4.3 Inhibition of Tuina on the TGF-β1/Smad3 pathway to attenuate MTrPs fibrosis

To further assess if Tuina can lessen MTrPs fibrosis by blocking the TGF-β1 pathway, the phase 2 of this study incorporated a TI group and a Tuina + TA group for rescue experiments. Research has established that the TGF-β1/Smad3 signaling pathway serves as the central process route through which TGF-β1 operates in living organisms [32].

Previous research indicates that TGF-β1 activated TGF-β receptors, leading to p-Smad3, which combined with Smad4 to form oligomeric complexes that moved into the nucleus, where they regulated the transcription of target genes, prompting myofibroblasts to produce significant amounts of collagen fibers and causing tissue fibrosis [33]. Interestingly, research has also discovered a strong link between the TGF-β1/Smad3 signaling pathway and tissue inflammation [34]. In individuals with chronic pain, the TGF-β1/Smad3 signaling pathway could work with NF-κB to strengthen inflammatory responses in tissues [35]. Studies indicate that the addition of TGF-β1 inhibitors has decreased tissue fibrosis accompanied by reduced inflammation, whereas administration of TGF-β1 agonists has promoted tissue fibrosis and inflammation [36, 37].

In the phase 2 of this study, intraperitoneal administration of oxymatrine, a TGF-β1 inhibitor, to rats with MTrPs effectively reduced inflammation and fibrosis in MTrPs, with Tuina exerting comparable therapeutic effects. These findings indicate that oxymatrine can indeed reduce the degree of MTrPs fibrosis, and the effect of Tuina is comparable to that of TI. Following intraperitoneal injection of SRI-011381 hydrochloride (a TGF-β1 agonist) in combination with Tuina intervention, levels of inflammation, fibrosis, TGF-β1, and p-Smad3 were all elevated in rats with MTrPs. These results indicate that SRI-011381 hydrochloride may activate the TGF-β1/Smad3 signaling pathway, enhance fibrosis in MTrPs, and attenuate the inhibitory effect of Tuina on MTrPs fibrosis. In summary, these findings demonstrate that Tuina inhibits the TGF-β1/Smad3 signaling pathway, thereby attenuating inflammation and fibrosis in MTrPs.

4.4 Limitations and prospects

TGF-β1 not only regulates fibrosis through Smad-dependent pathways but also accelerates fibrosis progression via non-Smad pathways, including extracellular signal-regulated kinase (ERK) activation, which promotes myofibroblast proliferation and extracellular matrix deposition [38], and the critical mediating role of the phosphatidylinositol 3-kinase (PI3K)/protein kinase B (AKT) signaling pathway [39]. Given that Tuina may inhibit MTrPs fibrosis via multiple targets and pathways, the current study only focused on the role of the TGF-β1/Smad3 signaling pathway in Tuina-mediated MTrPs treatment, without assessing changes in key molecules of the ERK or PI3K/AKT signaling pathways, which is a limitation of our study. This limited scope indicates that two critical questions cannot be comprehensively addressed: (i) whether Tuina activates TGF-β1 to induce ERK activation through non-Smad pathways, and (ii) whether Tuina inhibits the PI3K/AKT signaling pathway in MTrPs to regulate fibrosis, resulting in an incomplete interpretation of the underlying mechanisms of action.

In future research, we will systematically investigate the synergistic effects and interaction mechanisms of Tuina's regulation of multiple pathways from three dimensions: *in vivo*, *in vitro*, and temporal sequence, concentrating on the non-Smad3 signaling pathways of TGF-β1 and the PI3K/AKT signaling pathway. This will further refine the molecular network underlying Tuina's anti-MTrPs fibrosis effects and strengthen the depth and comprehensiveness of our studies.

5 Conclusion

This study demonstrates that Tuina can inactivate taut muscle bands by inhibiting the TGF-β1/Smad signaling pathway and reducing p-Smad3, thereby suppressing the formation of an inflammatory and fibrotic microenvironment at MTrPs. Our molecular findings offer a mechanistic explanation for these practices, supporting Tuina as a non-drug, low-risk alternative treatment for patients with chronic myofascial pain syndrome who cannot tolerate nonsteroidal anti-inflammatory drugs or injection treatments.

Fundings

Natural Science Foundation of China (82274676 and 82374613), and Program of Hunan Provincial Natural Science (2023JJ30458).

Ethical statement

All animal experiments were performed in compliance with China's national standards for animal welfare, and approval was obtained from the Laboratory Animal

Ethics Committee at Hunan University of Chinese Medicine (Ethics No. LL2021102004).

Author contributions

Liya Tang: writing – original draft, data curation, and software. Xiaowei Liu: project administration and methodology. Jiadong Zang: formal analysis and data curation. Yuqiao Zhang and Xiang Feng: software and methodology. Wu Li: project administration. Jiangshan Li: project administration and writing – review & editing. All authors approved the submission and take responsibility for this manuscript.

Competing interests

The authors declare no conflict of interest.

References

[1] NIAZI S, GANDOMI F, SOUFIVAND P, et al. The effect of tissue stretching and release strategies on neck muscles fatigue and pain intensity in office workers affected by chronic neck pain: a rater-blind, semi-experimental study. Health Science Reports, 2025, 8(4): e70748.

[2] ISHIKI H, HASUO H, MATSUDA Y, et al. Prevalence of myofascial pain syndrome and efficacy of trigger point injection in patients with incurable cancer: a multicenter, prospective observational study (MyCar study). Pain Medicine, 2022, 23(7): 1259–1265.

[3] GERWIN RD. A new unified theory of trigger point formation: failure of pre- and post-synaptic feedback control mechanisms. International Journal of Molecular Sciences, 2023, 24(9): 8142.

[4] FANG X, YIN YL, LUN HM, et al. Assessment of the effects of transforming growth factor beta1 (TGF-β1)-Smad2/3 on fibrosis in rat myofascial trigger points using point shear wave elastography. PeerJ, 2023, 11: e16588.

[5] BOCK-PEREDA A, CRUZ-SOCA M, GALLARDO FS, et al. Involvement of lysophosphatidic acid-LPA1-YAP signaling in healthy and pathological FAPs migration. Matrix Biology, 2024, 133: 103–115.

[6] LI X, QI T, ZHOU LW, et al. Isoliquiritigenin alleviates abnormal sarcomere contraction and inflammation in myofascial trigger points via the IL-17RA/Act1/p38 pathway in rats. Phytomedicine, 2025, 145: 156993.

[7] LOOMIS T, SMITH LR. Thrown for a loop: fibro-adipogenic progenitors in skeletal muscle fibrosis. American Journal of Physiology-Cell Physiology, 2023, 325(4): C895–C906.

[8] TAKIZAWA H, ARAKI Y, FUJISHIRO M, et al. Role of TGF-beta1 and TNF-alpha1 produced by neoplastic cells in the pathogenesis of fibrosis in patients with hematologic neoplasms. Journal of Clinical and Experimental Hematopathology, 2023, 63(2): 83–89.

[9] LI JW, NIU CX, AI HH, et al. TSP50 attenuates DSS-induced colitis by regulating TGF-β signaling mediated maintenance of intestinal mucosal barrier integrity. Advanced Science, 2024, 11(11): 2305893.

[10] REN LL, LI XJ, DUAN TT, et al. Transforming growth factor-β signaling: from tissue fibrosis to therapeutic opportunities. Chemico-Biological Interactions, 2023, 369: 110289.

[11] BAHN YJ, WANG YL, DAGUR P, et al. TGF-β antagonism synergizes with PPARγ agonism to reduce fibrosis and enhance beige adipogenesis. Molecular Metabolism, 2024, 90: 102054.

[12] CAO QW, PENG BG, WANG L, et al. Expert consensus on the diagnosis and treatment of myofascial pain syndrome. World Journal of Clinical Cases, 2021, 9(9): 2077–2089.

[13] LEW J, KIM J, NAIR P. Comparison of dry needling and trigger point manual therapy in patients with neck and upper back myofascial pain syndrome: a systematic review and meta-analysis. Journal of Manual & Manipulative Therapy, 2021, 29(3): 136–146.

[14] YANG ZJ, SA CL, YU TY, et al. Exploring the analgesic initiation mechanism of Tuina in the dorsal root ganglion of minor CCI rats via the TRPV1/TRPA1-cGMP pathway. Pain Research and Management, 2024, 2024: 2437396.

[15] LI CL. Observations on the achievements of massage therapy in the Qin and Han dynasties from the "*Huangdi Neijing*". Liaoning Journal of Traditional Chinese Medicine, 2003, 30(6): 453–454.

[16] DAYANıR IO, BIRINCI T, KAYA MUTLU E, et al. Comparison of three manual therapy techniques as trigger point therapy for chronic nonspecific low back pain: a randomized controlled pilot trial. The Journal of Alternative and Complementary Medicine, 2020, 26(4): 291–299.

[17] SATTAR MM, KHAN AH, KABIR MF, et al. Effectiveness of massage Gun versus myofascial release technique for releasing latent trigger points of the calf muscle: a protocol for randomized clinical trial. Physiotherapy Research International, 2025, 30(2): e70055.

[18] JIANG QR, FENG X, LIU D, et al. Pressing intervention promotes the skeletal muscle repair of traumatic myofascial trigger points in rats. Journal of Pain Research, 2021, 14: 3267–3278.

[19] HUANG QM, YE G, ZHAO ZY, et al. Myoelectrical activity and muscle morphology in a rat model of myofascial trigger points induced by blunt trauma to the vastus medialis. Acupuncture in Medicine, 2013, 31(1): 65–73.

[20] WANG HQ, CHEN FH, WANG L, et al. Biopharmaceutical and pharmacokinetic activities of oxymatrine determined by a sensitive UHPLC-MS/MS method. Current Pharmaceutical Biotechnology, 2022, 23(1): 148–157.

[21] LIU Y, GAO L, ZHAO XY, et al. Saikosaponin a protects from pressure overload-induced cardiac fibrosis via inhibiting fibroblast activation or endothelial cell EndMT. International Journal of Biological Sciences, 2018, 14(13): 1923–1934.

[22] ZENG YJ, DU CJ, HUANG C, et al. Diagnosis of neck pain using a soft tissue force-displacement testing system. Chinese Journal of Biomedical Engineering, 2005(5): 583–586.

[23] HU JT, TONG HX, ZHANG JL, et al. Acupotomy for musculoskeletal pain: exploring therapeutic potential and future directions. Journal of Pain Research, 2025, 18: 3027–3036.

[24] DEWI N, MEILIANA A, DEFI I, et al. Targeted therapy for skeletal muscle fibrosis: regulation of myostatin, TGF-β, MMP, and TIMP to maintain extracellular matrix homeostasis. Biologics: Targets and Therapy, 2025, 19: 213–229.

[25] VENUGOPAL H, HANNA A, HUMERES C, et al. Properties and functions of fibroblasts and myofibroblasts in myocardial infarction. Cells, 2022, 11(9): 1386.

[26] ANTAR SA, ASHOUR NA, MARAWAN ME, et al. Fibrosis: types, effects, markers, mechanisms for disease progression, and its relation with oxidative stress, immunity, and inflammation. International Journal of Molecular Sciences, 2023, 24(4): 4004.

[27] WOHLGEMUTH RP, SRIRAM S, HENRICSON KE, et al. Strain-dependent dynamic re-alignment of collagen fibers in skeletal muscle extracellular matrix. Acta Biomaterialia, 2024, 187: 227–241.

[28] LEI BK, ZHAO S, XU T, et al. TGF-β1/ERK/CTGF pathway involved in effect of acupuncture on exercise-induced skeletal muscle fibrosis. Acupuncture Research, 2021, 46(4): 306–311.

[29] LODYGA M, HINZ B. TGF-β1–A truly transforming growth factor in fibrosis and immunity. Seminars in Cell & Developmental Biology, 2020, 101: 123–139.

[30] QIU YF, SONG XD, LIU Y, et al. Application of recombinant TGF-β1 inhibitory peptide to alleviate isoproterenol-induced cardiac fibrosis. Applied Microbiology and Biotechnology, 2023, 107(20): 6251–6262.

[31] BAIK JE, PARK HJ, KATARU RP, et al. TGF-β1 mediates pathologic changes of secondary lymphedema by promoting fibrosis and inflammation. Clinical and Translational Medicine, 2022, 12(6): e758.

[32] ZHANG Q, GENG M, LI K, et al. TGF-β1 suppresses the T-cell response in teleost fish by initiating Smad3- and Foxp3-mediated transcriptional networks. Journal of Biological Chemistry, 2023, 299(2): 102843.

[33] YANG ZS, ZHANG H, YIN MH, et al. TGF-β1/Smad3 upregulates UCA1 to promote liver fibrosis through DKK1 and miR18a. Journal of Molecular Medicine, 2022, 100(10): 1465–1478.

[34] WU H, FENG YY, ZHANG RY, et al. 6: 2 chlorinated polyfluoroalkyl ether sulfonate (F–53B) induced nephrotoxicity associated with oxidative stress, inflammation and fibrosis in mice. Chemico-Biological Interactions, 2025, 405: 111290.

[35] LEI ZG, TANG R, WU Y, et al. TGF-β1 induces PD-1 expression in macrophages through SMAD3/STAT3 cooperative signaling in chronic inflammation. JCI Insight, 2024, 9(7): e165544.

[36] LI DL, ZHANG J, YUAN SY, et al. TGF-β1 peptide-based inhibitor P144 ameliorates renal fibrosis after ischemia–reperfusion injury by modulating alternatively activated macrophages. Cell Proliferation, 2022, 55(10): e13299.

[37] CHEN CJ, CHEN JJ, WANG Y, et al. *Ganoderma lucidum* polysaccharide inhibits HSC activation and liver fibrosis via targeting inflammation, apoptosis, cell cycle, and ECM-receptor interaction mediated by TGF-β/Smad signaling. Phytomedicine, 2023, 110: 154626.

[38] WANG Y, GAO JF, SUN LQ, et al. Jiawei Simiao Yong'an Fang stimulates the healing of acute radiation-induced cutaneous wounds through MAPK/ERK pathway. Journal of Ethnopharmacology, 2023, 306: 116180.

[39] NI YF, ZHANG HM, XIAN QW, et al. Rf_xCas13d-mediated inhibition of *Circ1647* alleviates renal fibrosis via PI3K/AKT signaling pathway. Renal Failure, 2024, 46: 2331612.

(Editor-in-Charge Siyi Wei)

基于 TGF-β1/Smad3 信号通路探讨推拿按法抑制激痛点纤维化的作用机制

唐丽亚[a], 刘小卫[a], 臧家栋[b], 张玉乔[a], 冯祥[a], 李武[a], 李江山[a*]

a. 湖南中医药大学针灸推拿与康复学院, 湖南 长沙 410208, 中国
b. 湖南中医药大学科技处, 湖南 长沙 410208, 中国

【摘要】目的 探究推拿按法是否通过调节转化生长因子（TGF）-β1/Smad3 信号通路来减轻激痛点的纤维化症状，从而去活化激痛点。**方法** 本研究分为两阶段，第一阶段将 27 只无特定病原体（SPF）级的雌性 SD 大鼠随机分为对照 1 组、模型 1 组和推拿 1 组，其中模型 1 组和推拿 1 组进行为期 8 周的钝性击打和离心运动。造模成功后，对推拿 1 组大鼠左下肢内侧的结节或者条索状紧绷带进行按法干预。通过机械痛阈（PPT）和软组织张力（STT）评估大鼠疼痛敏感性和组织硬度。采用苏木精-伊红（HE）染色和 Masson 染色观察大鼠肌肉组织结构和纤维化情况，采用酶联免疫吸附测定（ELISA）检测大鼠肌肉组织中炎症因子水平，采用免疫荧光和蛋白印迹法（WB）检测平滑肌肌动蛋白（α-SMA）、Ⅲ型胶原和 TGF-β1 的表达。第二阶段将 45 只 SPF 级雌性 SD 大鼠随机分为对照 2 组、模型 2 组、推拿 2 组、TGF-β1 抑制剂（TI）组和推拿 + TGF-β1 激动剂（TA）组，除对照 2 组外，其余各组均进行造模处理。造模成功后，推拿 2 组进行按法干预，TI 组腹腔注射 TGF-β1 抑制剂苦参碱，推拿 + TA 组先腹腔注射 TGF-β1 激动剂 SRI-011381 盐酸盐后进行按法干预。通过 WB 检测Ⅰ型胶原、Ⅲ型胶原、TGF-β1 和磷酸化-Smad3（p-Smad3）/Smad3 的表达水平。**结果** 第一阶段研究结果发现，推拿可显著提高大鼠激痛点的 PPT 与 STT（$P < 0.01$），逆转大鼠激痛点肌肉纤维排列紊乱、肌细胞形态异常及纤维化加重等病理损伤。此外，模型 1 组大鼠激痛点组织中，白细胞介素（IL）-1β、IL-6、核因子（NF）-κB、肿瘤坏死因子（TNF）-α 等炎症因子和纤维化标志物（α-SMA、Ⅰ型胶原、Ⅲ型胶原）的表达升高，经推拿干预后均显著下调（$P < 0.05$ 或 $P < 0.01$），说明推拿的治疗作用与激痛点局部炎症及纤维化水平的改善直接相关。第二阶段结果发现，TI 组和推拿 2 组大鼠激痛点组织相较于模型 2 组，TGF-β1 和 p-Smad3/Smad3 的表达水平降低，IL-1β、IL-6、NF-κB、TNF-α 等炎症因子和纤维化标志物（α-SMA、Ⅰ型胶原和Ⅲ型胶原）表达水平也下降（$P < 0.05$ 或 $P < 0.01$）。当联合使用 TGF-β1 通路激动剂时，推拿的治疗效应被显著削弱，激痛点局部 TGF-β1 及 p-Smad3/Smad3 表达水平回升，纤维化与炎症反应再次加剧（$P < 0.05$ 或 $P < 0.01$）。**结论** 推拿可有效减轻大鼠激痛点组织中的炎症反应和纤维化，其机制与抑制 TGF-β1/Smad3 信号通路密切相关，该通路在推拿调控激痛点纤维化过程中发挥关键作用。

【关键词】推拿；按法；炎症；激痛点；纤维化；转化生长因子-β1；磷酸化-Smad3